

Preparation and properties of $\text{Al}_2\text{O}_3/\text{Ni}$ composite from NiAl_2O_4 spinel by in situ reaction sintering method

Toshihiro Isobe^{a,*}, Keiji Daimon^a, Kazunori Ito^a, Takashi Matsubara^a,
Yasuo Hikichi^a, Toshitaka Ota^b

^a Department of Materials Science and Engineering, Nagoya Institute of Technology, Gokiso, Showa, Nagoya 466-8555, Japan

^b Ceramics Research Laboratory, Nagoya Institute of Technology, 10-6-29 Asahigaoka, Tajimi, Gifu 507-0071, Japan

Received 23 January 2006; received in revised form 18 February 2006; accepted 31 March 2006

Available online 28 August 2006

Abstract

$\text{Al}_2\text{O}_3/\text{Ni}$ nano composites were prepared from NiAl_2O_4 spinel by in situ reaction sintering method. The starting materials of Al_2O_3 –NiO powder were synthesized by thermal decomposition of precipitates prepared from aluminum sulfate and nickel sulfate. The specific surface area of the Al_2O_3 –NiO powder was $>36 \text{ m}^2/\text{g}$. The $\text{Al}_2\text{O}_3/\text{Ni}$ composites were obtained by firing the starting material buried in a carbon bed at 1500°C for 1 h. The resulting $\text{Al}_2\text{O}_3/\text{Ni}$ composites have relative densities $>96\%$ (0–40 mol% Ni). Nickel grains dispersed homogeneously in the microstructure, accounting for 10% of within the grains and 90% at grain boundaries. The average particle size of the former nickel grains was 150 nm while that of the latter grains was 300 nm. The maximum three-point bending strength was 408 MPa at 10 mol% Ni sample and the maximum fracture toughness was $9.9 \text{ MPa m}^{1/2}$ at 40 mol% Ni sample. The Vickers hardness decreased slightly with increasing Ni content and this change is in good agreement with individual mixture rule.

© 2006 Elsevier Ltd and Techna Group S.r.l. All rights reserved.

Keywords: B. Nano composites; C. Mechanical properties; D. Al_2O_3 ; E. Structural applications

1. Introduction

Alumina is a widely used ceramics for structural applications because it has high mechanical properties, thermal stability and corrosion resistant properties [1]. However, alumina ceramics are weak brittle with regard to fracture toughness. Nano composites are thought to be one of the effective ways to improve the mechanical properties [2]. The fracture strength of alumina is reported to be clearly enhanced by $\text{Al}_2\text{O}_3/\text{Ni}$ nano composites [3–8]. To prepare such ceramics/metal nano composites, many problems still remain. The first issue is the difference of densities between ceramic and metal powders. Conventional mechanical mixing using a ball mill is inadequate for preparation of such nano composites having homogeneous microstructure. The

second point is the difficulty in dispersing nano metal particles in the ceramic matrix because of their high surface energy.

To solve these problems, several attempts have been reported in the literature. Sekino et al. have prepared $\text{Al}_2\text{O}_3/\text{Ni}$ nano composites by hot-pressing of Al_2O_3 and Ni mixed powders under argon atmosphere [3,4]. Lu et al. have prepared $\text{Al}_2\text{O}_3/\text{Ni}$ nano composites by hot-pressing of nano sized nickel particles coated with alumina precursor by heterogeneous precipitation method [5]. These nano composites show homogeneous microstructures and high mechanical properties. However, they require the use of hot-pressing method. For mass production, pressure-less sintering is preferable to prepare nano composites [7,8].

The in situ reaction sintering method [9], forming nano size grains of secondary phase by thermal decomposition of complex compound during reactive sintering, shows potential to obtain nano composites by pressure-less sintering. This process is thought to have the following advantage: (1) similar densities of starting materials as a monophase compound, (2) small secondary grains are formed by thermal decomposition of starting materials, and (3) high sinterability due to the small grain size.

* Correspondence to: Department of Metallurgy and Ceramics Science, Tokyo Institute of Technology, 2-12-1 O-okayama, Meguro, Tokyo 152-8552, Japan. Tel.: +81 3 5734 3355; fax: +81 3 5734 3355.

E-mail address: isobe@rmat.ceram.titech.ac.jp (T. Isobe).

For preparation of $\text{Al}_2\text{O}_3/\text{Ni}$ nano composites, $\text{Al}_2\text{O}_3\text{--NiO}$ powder is used as the raw material because it can be converted to $\alpha\text{-Al}_2\text{O}_3$ and Ni, under reducing atmosphere. In this study, $\text{Al}_2\text{O}_3/\text{Ni}$ nano composites were prepared from the $\text{Al}_2\text{O}_3\text{--NiO}$ powder by in situ reaction sintering method, and their mechanical properties were investigated.

2. Experimental procedure

$\text{Al}_2\text{O}_3\text{--NiO}$ co-precipitated powders were prepared by the water solution heating method developed by Daimon et al. [10]. High purity aluminum sulfate ($\text{Al}_2(\text{SO}_4)_3 \cdot 14\text{--}18\text{H}_2\text{O}$, Hayashi Pure Chemical Ind., Japan) and high purity nickel sulfate ($\text{NiSO}_4 \cdot 6\text{H}_2\text{O}$, Kishida Chemical, Japan) (0–50 mol%) were dissolved and mixed in water for 2 h. The obtained solution was rapidly dried by microwave (MR-P1510, Hitachi, Japan), calcined at 900 °C for 4 h to remove sulfate and further calcined at 1250 °C for 1 h. The obtained powder was wet ball milled in an ethanol for 48 h and dried at 110 °C for 2 h. The resulting powder was uniaxially pressed at 30 MPa for 3 min to prepare disks (15 mm \varnothing , 5 mm in height) or plates (55 mm \times 45 mm \times 6 mm), and cold isostatic pressing (CIP) at 100 MPa for 10 min. They were sintered at 1500 °C for 1 h in a carbon powder bed. To investigate the phase change during sintering, the disk samples after the CIP process were heated at various temperatures for 1 h in carbon powder.

The phases formed in the powder and composite samples were examined by X-ray diffractometry (XRD) using Cu K α radiation (RAD-B, Rigaku, Japan). The specific surface area of the powder sample is determined by B.E.T. method using nitrogen (NOVA1000, Yuasa Ionics Inc., Japan). The relative densities of the samples were measured by the Archimedes technique using water. The three-point bending strengths of the sintered test pieces (3 mm \times 4 mm \times 40 mm) were measured with a span length of 30 mm and crosshead speed of 0.5 mm/min (AGS-5kND, Shimadzu, Japan). The surfaces were polished with 3 and 6 μm diamond pastes. The average bending strength was obtained from measurements of 10 samples. The Vickers micro hardness was measured using a Vickers hardness tester (AVK-A, Akashi, Japan) with a 9.8–98 N load on the polished surface. The fracture toughness was evaluated by indentation fracture (IF) method. The micro-structure of the sample surface was observed using a scanning electron microscope (SEM) (JSM-5200, JEOL, Japan) and transmission electron microscope (TEM) (JEM-2010, JEOL, Japan). The average grain size was evaluated by the intercept method.

3. Results and discussion

3.1. Characterization of $\text{Al}_2\text{O}_3\text{--NiO}$ powder

Fig. 1 shows the XRD patterns of the obtained $\text{Al}_2\text{O}_3\text{--NiO}$ powders. The powder with low nickel content shows only $\alpha\text{-Al}_2\text{O}_3$ peaks. By contrast, the powders containing 10 and 20 mol% Ni show peaks assigned to $\alpha\text{-Al}_2\text{O}_3$ and NiAl_2O_4 spinel while those containing ≥ 30 mol% Ni show only NiAl_2O_4 spinel

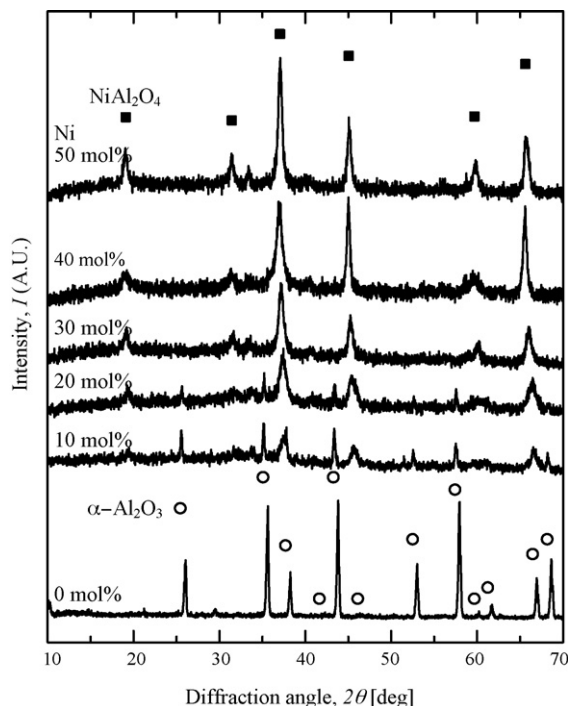


Fig. 1. XRD pattern of the $\text{Al}_2\text{O}_3\text{--Ni}$ solid solution powders after calcining at 1250 °C for 1 h.

peaks. Since the solid solution range of NiAl_2O_4 spinel is reported to be >26 mol% at 1390 °C [11], the XRD results of the present powders were in good agreement with reported phase diagram. Formation of Ni–Al spinel is very effective to avoid heterogeneity of the composites due to the density difference because >26 mol% Ni powders consisted of a single phase. Although the powders ($\text{Ni} \leq 26$ mol%) consisted of two phases, the densities of $\alpha\text{-Al}_2\text{O}_3$ (4.0 g/cm 3) and NiAl_2O_4 (4.4 g/cm 3) are similar. The specific surface area of $\alpha\text{-Al}_2\text{O}_3$ was 7.6 m 2 /g but those of the Ni containing powders were 36–53 m 2 /g, much higher specific surface areas. This increase in surface area is attributed to the cation dope effect [12]. The average particle size of the Ni containing powders calculated from the specific surface area is about 15 nm, being sufficiently small for in situ reaction sintering. Therefore, the $\text{Al}_2\text{O}_3\text{--NiO}$ powders synthesized show adequate chemical compositions and high specific surface areas as expected.

3.2. Preparation of $\text{Al}_2\text{O}_3/\text{Ni}$ composites

The XRD patterns of the samples (50 mol% Ni) heated at various temperatures are shown in Fig. 2. The samples heated at 500 and 600 °C show only NiAl_2O_4 spinel peaks. Formation of NiO found by heating at >700 °C and this NiO was reduced to Ni metal at >800 °C. Transition Al_2O_3 formed by decomposition of spinel transformed to $\alpha\text{-Al}_2\text{O}_3$ at ≥ 1300 °C, and the obtained sample is consisted of $\alpha\text{-Al}_2\text{O}_3$ and Ni. These phase change is similar to what has been previously reported [10]. The initial stage of sintering occurred from 1300 °C in the present sample and the decomposition of NiAl_2O_4 was already completed. It is thought that when the decomposition occurs

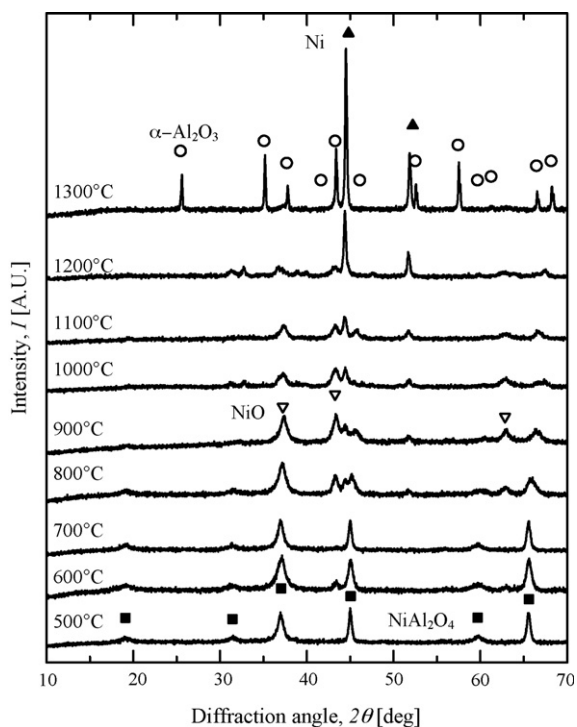


Fig. 2. XRD pattern of the NiAl_2O_4 after reduction in carbon at various temperatures for 1 h.

at a later stage, the composites would have the residual stress and cause cracks in the microstructure. The XRD patterns of the composites heated at 1500 °C for 1 h in a carbon bed (Fig. 3) show that all the samples consisted of only two phases, $\alpha\text{-Al}_2\text{O}_3$ and Ni.

The relative densities and the grain sizes of alumina matrix in the present samples after sintering at 1500 °C for 1 h in a

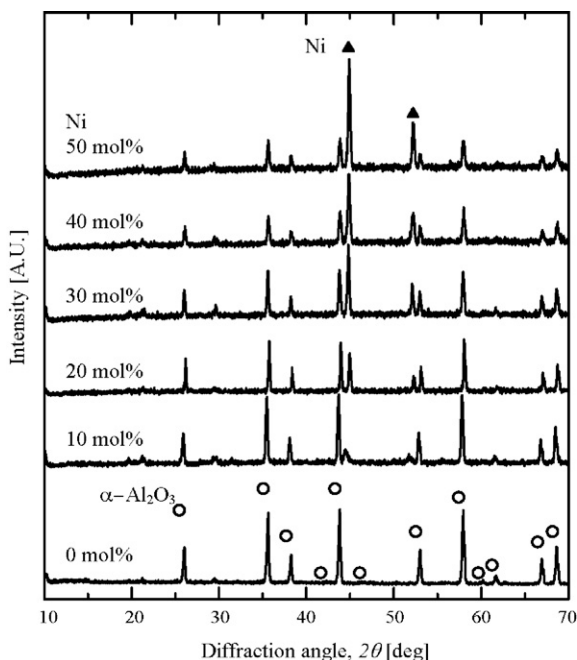


Fig. 3. XRD pattern of the $\text{Al}_2\text{O}_3/\text{Ni}$ composites after sintering in carbon at 1500 °C for 1 h.

Table 1

The properties of the $\text{Al}_2\text{O}_3\text{-Ni}$ solid solution powders

Ni content (mol%)	Crystalline phase	Specific surface area (m^2/g)
0	$\alpha\text{-Al}_2\text{O}_3$	7.6
10	$\alpha\text{-Al}_2\text{O}_3$, NiAl_2O_4	42.3
20	$\alpha\text{-Al}_2\text{O}_3$, NiAl_2O_4	53.1
30	NiAl_2O_4	50.3
40	NiAl_2O_4	45.1
50	NiAl_2O_4	35.6

carbon bed are listed in Table 1. The relative densities of ≤ 40 mol% Ni samples are higher than that of the 50 mol% nickel containing sample. This slight decrease is thought to be due to the densification suppression by Ni grains. The grain sizes of alumina in the resulting obtained composites decrease from 1.95 to 0.91 μm with increasing Ni content. It is proposed that Ni grains located at grain boundaries suppressed grain growth of matrix alumina. Fig. 4 shows SEM micrographs of the 10 mol% (a) and 50 mol% (b) Ni composites. The microstructures of both samples show homogeneous dispersion of Ni grains, surrounding the matrix of alumina grains. Fig. 5 shows TEM micrographs of the 10 mol% Ni composite. Only a small amount of Ni grains (10%) is located inter-granularly and the remaining 90% are located at the grain boundaries and the triple junctions. The average Ni grain sizes located at intra- and inter-alumina grains are 300 and 150 nm, respectively. In situ decomposition method is, therefore, an excellent method to

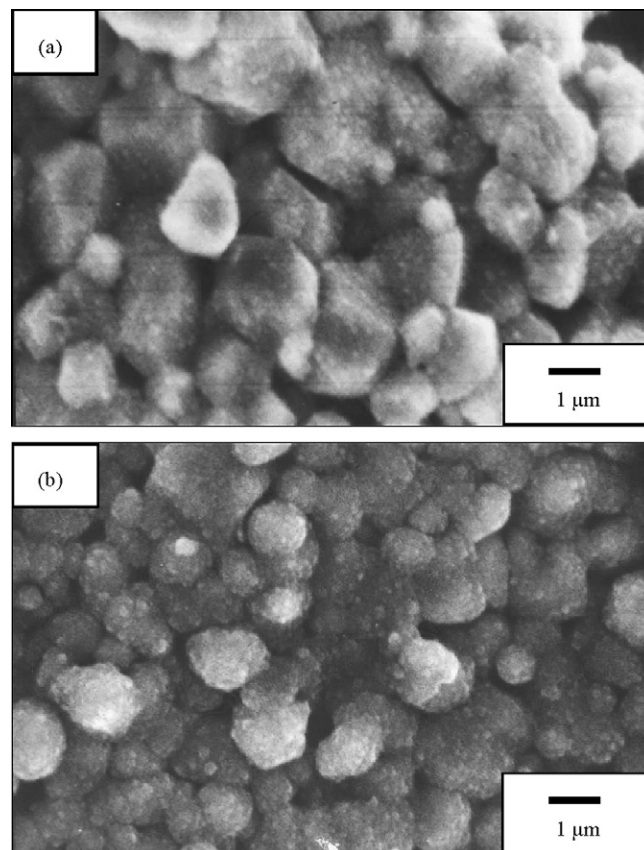


Fig. 4. SEM micrographs of the (a) 10 mol% and (b) 50 mol% nickel containing composites.

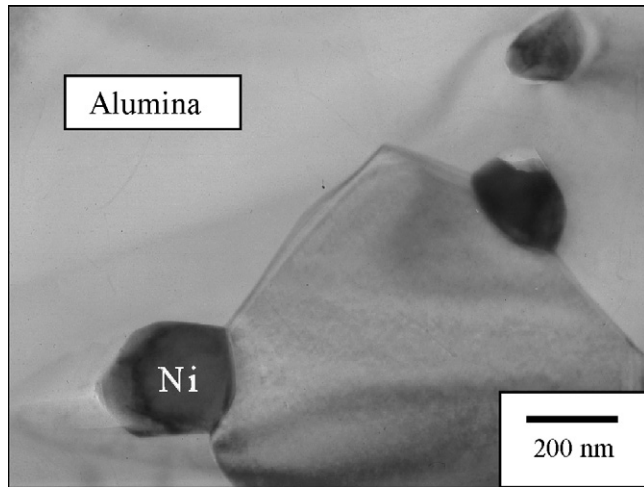


Fig. 5. TEM micrographs of the 10 mol% nickel containing specimen.

fabricate $\text{Al}_2\text{O}_3/\text{Ni}$ composites with homogeneously dispersing nano Ni grains in the alumina matrix.

3.3. Mechanical properties

Fig. 6 shows three-point bending strengths of the resulting $\text{Al}_2\text{O}_3/\text{Ni}$ composites. The strength increases up to 408 MPa by dispersing 10 mol% Ni, which is only 2.8 vol%. However, Table 2 the strength decreases with increasing Ni content. The maximum strength of the composites is generally obtained by mixing 5–10 vol% of the second phase. By contrast, the present composites show the maximum strength at much lower Ni content. This may be achieved by homogeneous dispersion of nano Ni grains. Critical flaw size of the composites is thought to relate with grain size of matrix alumina. However, the fracture strengths of the composites do not increase but decrease with decreasing of alumina grain size. It is, therefore, necessary to consider another mechanism to explain the present results.

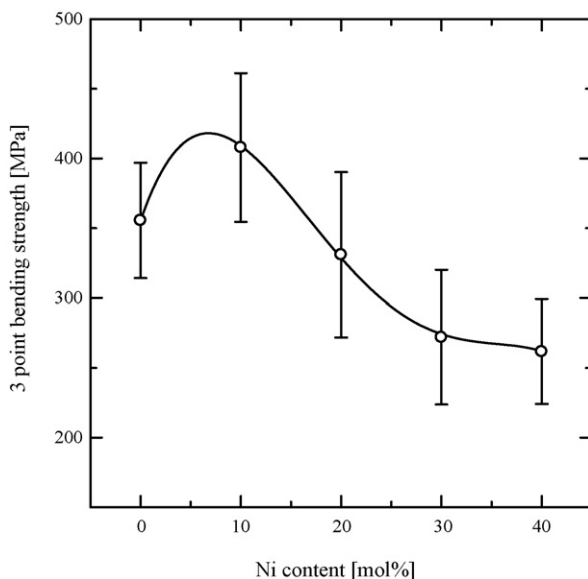


Fig. 6. Relationship between nickel content and three-point bending strength of the nano composite.

Table 2

The relative density and the alumina grain size of the $\text{Al}_2\text{O}_3/\text{Ni}$ composites

Ni content (mol%)	Ni content (vol%)	Relative density (%)	Average alumina grain size (μm)
0	0	96	1.95
10	2.8	96	1.49
20	6.1	97	1.02
30	10.0	97	0.96
40	14.7	97	0.94
50	20.6	92	0.91

Many strengthening and toughening mechanisms were proposed in the literature. Sternizke divided the mechanisms into three groups: (1) reduction of critical flaw size, (2) increase of fracture toughness and (3) grain boundary strengthening [13]. Choi et al. suggested another mechanism, which is expansion of frontal process zone size [14]. From the microstructures of the composites, the grain boundary strength of the 50 mol% Ni containing composite is observed to be clearly weaker than that of the 10 mol% Ni containing composite. To expand the size of frontal process zone, Ni grains should be present inside the alumina grains. Since 10% of Ni grains in the composites fit this condition, the strengthening mechanism of the resulting composites is attributed to the expansion of frontal process zone size. In contrast, the decreasing of the strength of composites ≥ 20 mol% Ni is attributed to the grain boundary weakening effect of the composites.

Fig. 7 shows changes of fracture toughness and Vickers micro hardness as a function of Ni content in the composites. The fracture toughness of 0 mol% Ni sample was $2.6 \text{ MPa m}^{1/2}$. This value drastically increases with increasing Ni content in the samples and reached up to $9.9 \text{ MPa m}^{1/2}$ by loading 40 mol% Ni. The enhancement of fracture toughness is attributed to the Ni grains, acting either as crack deflection points or stopping the crack propagation due to its ductility. The Vickers micro hardness shows a slight decrease with increase Ni content.

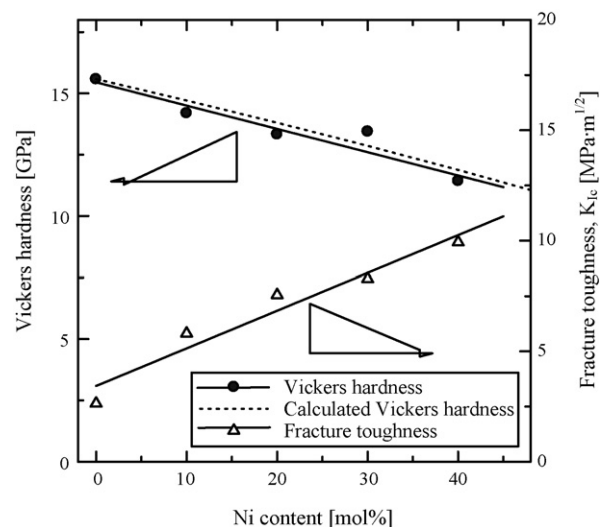


Fig. 7. Vickers hardness and fracture toughness of the $\text{Al}_2\text{O}_3/\text{Ni}$ composites as a function of Ni content.

The Vickers micro hardness of the composites (Hv_{comp}) was calculated using mixture rule from the individual Vickers micro hardness of alumina value (15.2 GPa) and Ni (5.0 GPa).

$$Hv_{\text{comp}} = \sum_i V_i Hv_i$$

where V_i and Hv_i are the volume fraction and micro hardness of each phase. The micro calculated Vickers hardness value (dotted line) shown in Fig. 7 shows good agreement with the observed data. This may mean that each phase behaves individually in the nano composites.

4. Summary

$\text{Al}_2\text{O}_3/\text{Ni}$ nano composites were prepared by an in situ reaction sintering method using co-precipitated $\text{Al}_2\text{O}_3\text{--NiO}$ powders. The starting materials of $\text{Al}_2\text{O}_3\text{--NiO}$ powders were synthesized from solution dissolving aluminum sulfate and nickel sulfate. Their grain sizes were about 15 nm and suitable as the raw material for the in situ reaction sintering method. $\text{Al}_2\text{O}_3/\text{Ni}$ composites were prepared by heating under reducing atmosphere using a carbon bed. The resulting $\text{Al}_2\text{O}_3/\text{Ni}$ composites show good sinterability, reaching almost full density with a wide range of Ni contents. Nickel grains dispersed homogeneously in the microstructure, 10% of the Ni grains intra-granularly and 90% inter-granularly at the grain boundaries and the triple junctions. The average grain sizes of the inter- and intra-granularly Ni grain size were 300 and 150 nm, respectively. The grain sizes of alumina in the samples decreased from 1.95 to 0.91 μm with increasing Ni contents. The three-point bending strength showed the maximum of 408 MPa in the 10 mol% Ni sample (2.8 vol% Ni), apparently lower Ni content than the previous reports. The fracture toughness of the composites drastically increased from 2.6 $\text{MPa m}^{1/2}$ in the monolithic alumina to 9.9 $\text{MPa m}^{1/2}$ in the 40 mol% Ni composite. The Vickers micro hardness decreased slightly with increasing Ni content, in good agreement with individual mixture rule. This in situ reaction sintering technique is applicable to a variety of nano composites.

Acknowledgements

The authors thank Professors K. Okada and J.S. Cross of Tokyo Institute of Technology for critical reading and editing of this manuscript.

References

- [1] R.G. Munro, Evaluated material properties for a sintered α -alumina, *J. Am. Ceram. Soc.* 80 (8) (1997) 1919–1928.
- [2] K. Niihara, New design concept of structural ceramic/ceramic nanocomposites, *J. Ceram. Soc. Jpn.* 99 (10) (1991) 974–982.
- [3] T. Sekino, T. Nakajima, K. Niihara, Mechanical and magnetic properties of nickel dispersed alumina-based nanocomposite, *Mater. Lett.* 29 (1–3) (1996) 165–169.
- [4] T. Sekino, T. Nakajima, S. Ueda, K. Niihara, Reduction and sintering of a nickel-dispersed-alumina composite and its properties, *J. Am. Ceram. Soc.* 80 (5) (1997) 1139–1148.
- [5] J. Lu, L. Gao, J. Sun, L. Gui, L. Guo, Effect of nickel content on the sintering behavior, mechanical and dielectric properties of $\text{Al}_2\text{O}_3/\text{Ni}$ composites from coated powders, *Mater. Sci. Eng. A293* (1) (2000) 223–228.
- [6] G.J. Li, X.X. Huang, K.J. Guo, Fabrication and mechanical properties of $\text{Al}_2\text{O}_3/\text{Ni}$ composite from two different powder mixtures, *Mater. Sci. Eng. A352* (1) (2003) 23–28.
- [7] R.Z. Chen, W.H. Tuan, Pressureless sintering of $\text{Al}_2\text{O}_3/\text{Ni}$ nanocomposites, *J. Eur. Ceram. Soc.* 19 (4) (1999) 463–468.
- [8] M. Lieberthal, W.D. Kaplan, Processing and properties of Al_2O_3 nanocomposites reinforced with sub-micron Ni and NiAl_2O_4 , *Mater. Sci. Eng. A302* (1) (2001) 83–91.
- [9] Y. Suzuki, N. Kondo, T. Ohji, Reactive synthesis of a porous calcium zirconate/spinel composite with idiomorphic spinel grains, *J. Am. Ceram. Soc.* 86 (7) (2003) 1128–1131.
- [10] K. Daimon, T. Isobe, Y. Hikichi, T. Ota, Partial reduction of reactive NiAl_2O_4 spinel prepared from a sulfate solid solution, *Nippon Kagaku Kaishi* 2002 (2) (2002) 195–199 (in Japanese).
- [11] K.P. Trumble, M. Rühle, The thermodynamics of spinel interphase formation at diffusion-bonded $\text{Ni}/\text{Al}_2\text{O}_3$ interfaces, *Acta Metall. Mater.* 39 (8) (1991) 1915–1924.
- [12] S. Rossignol, C. Kappenstein, Effect of doping elements on the thermal stability of transition alumina, *Int. J. Inorg. Mater.* 3 (1) (2001) 51–58.
- [13] M. Sternitzke, Review: structural ceramic nanocomposites, *J. Eur. Ceram. Soc.* 17 (9) (1997) 1061–1082.
- [14] S.M. Choi, H. Awaji, Nanocomposites—a new material design concept, *Sci. Tech. Adv. Mater.* 6 (1) (2005) 2–10.